



# Journal of Applied Sciences

ISSN 1812-5654

**science**  
alert

**ANSI***net*  
an open access publisher  
<http://ansinet.com>

## Comparison of Mechanical Properties and Magnetic Properties of $Mn_{0.8}Zn_{0.2}Fe_2O_4$ Synthesized by Conventional Ball Milling and Self Combustion Method

<sup>1</sup>P. Puspitasari, <sup>2</sup>N. Yahya, <sup>2</sup>N.A.M. Zabidi and <sup>1</sup>N.A. Ahmad

<sup>1</sup>Department of Electrical and Electronic Engineering,

<sup>2</sup>Department of Fundamental and Applied Science, Universiti Teknologi PETRONAS,  
Bandar Seri Iskandar, 31750 Bandar Seri Iskandar, Malaysia

**Abstract:** Manganese zinc ferrite is a soft ferrite material that has been used in many applications including catalyst. Therefore, studies on the mechanical and magnetic properties are very important in order to enhance the performance of the catalyst. This study will compare the mechanical and magnetic properties of manganese zinc ferrite ( $Mn_{0.8}Zn_{0.2}Fe_2O_4$ ) synthesized by conventional ball milling and self combustion methods. Microhardness Vickers and Impedance Analyzer were used to investigate. Morphology and structure of  $Mn_{0.8}Zn_{0.2}Fe_2O_4$  were characterized by using X-Ray Diffraction, Field Emission Scanning Electron Microscope (FESEM) and Energy Dispersive X-Ray (EDX). The catalyst characterization was performed using a Temperature Program Reduction (TPR). It has been shown that  $Mn_{0.8}Zn_{0.2}Fe_2O_4$  synthesized by self combustion method has better mechanical properties (75.83 HVN) and magnetic properties with a superior initial permeability ( $2.5 \times 10^3$ ) and Relative Loss Factor (0.03) compared to conventional ball milling method.

**Key words:** Mechanical properties, magnetic properties,  $Mn_{0.8}Zn_{0.2}Fe_2O_4$ , conventional ball milling, self combustion

### INTRODUCTION

MnZn-ferrites are considered as one of the great important soft ferrite ceramic materials. This type of ceramics find extensive applications in electronic and telecommunication industry and catalyst. Spinel ferrites combine interesting soft magnetic properties with rather high electrical resistivities (Emad *et al.*, 2008). Because of the chemical composition and crystal structure of Mn-Zn ferrite, this material has a high initial permeability, saturation magnetization and a relatively low eddy current losses compared with alloy cores.

Various processing techniques including conventional and nonconventional have been developed for the synthesis of ferrites. However, each one of these techniques has its specific limitations. Non-conventional techniques such as co-precipitation, thermal decomposition, sol-gel and hydrothermal, self-propagating high temperature synthesis (SHS) and other wet chemical techniques were widely used. (Nalbandian *et al.*, 2008). The main disadvantage concerns economic and environmental. Therefore, the manufacturing of near fully dense manganese zinc ferrites through minimum number of steps with high magnetic properties will be the focus of this research.

The mechanical and magnetic properties of manganese zinc ferrites depend on their microstructure.

The grain size and porosity of the sample will affect the strength performance of the material. One of the main problems during conventional sintering of manganese zinc ferrites is the elimination of porosity. It is well known that the domains structure of magnetic materials is affected by crystal structure, saturation magnetization, magnetocrystalline anisotropy and magnetostriction as well as the size and shape of grains, porosity and crystal defects, which are determined by the processing route (Kazemi and Fantozzi, 2006). Among many of the novel mechanical properties of nanomaterials, hardness has been discovered from many nanomaterials system. Hence this study will focus on the hardness testing for mechanical properties and permeability testing as indicators for magnetic properties of  $Mn_{0.8}Zn_{0.2}Fe_2O_4$  nanoparticle.

Currently many researcher have discussed the magnetic and mechanical properties of manganese zinc ferrite (Zuo *et al.*, 2005; Sun *et al.*, 2009; Ni and Lwin, 2008). Magnetic properties of manganese ferrite which is the saturation magnetization depend on the chemical composition and oxygen pressure (Zuo *et al.*, 2005). Meanwhile, other researchers have found that the permeability of MnZn Ferrites increase by dopping with NiO (Sun *et al.*, 2009). It has been reported that the permeability maximum for  $M_{n(1-x)}Zn_{(x)}Fe_2O_4$  was for ZnFerrite with the composition of 0.25 (Ni and Lwin, 2008).

Study on the mechanical properties of manganese zinc ferrite was reported by some researchers (Kazemi and Fantozzi, 2006; Berdikov *et al.*, 1983; Baumgartner *et al.*, 1997). Mechanical properties including internal friction and shear modulus of manganese zinc ferrite has been reported by Kazemi and Fantozzi (2006). It has been found that internal friction and shear modulus depend on the motion of the domain wall and currie temperature. It was reported that the load on indenting constitutes a local stress raiser and brittle fracture of material (Berdikov *et al.*, 1983). Comparison study of the mechanical and magnetic properties of manganese zinc ferrite has been discussed (Baumgartner *et al.*, 1997). It has been reported that tensile strength, toughness, and thermal shock resistivity are determined by grain and pore size (Baumgartner *et al.*, 1997). This study will analyze the comparison on mechanical properties (hardness) and magnetic properties (permeability and relative loss factor) of  $Mn_{0.8}Zn_{0.2}Fe_2O_4$  by ball milling method and self combustion technique. The catalyst characterization will be conducted by using TPDR0 1100 series to study the activation energy of  $Mn_{0.8}Zn_{0.2}Fe_2O_4$ .

**MATERIALS AND METHODS**

**Preparation of  $Mn_{0.8}Zn_{0.2}Fe_2O_4$  by ball milling method:**

The precursor for  $Mn_{0.8}Zn_{0.2}Fe_2O_4$  was prepared by solid state reaction consisting of three oxides namely Zinc Oxide (ZnO), Manganese Oxide (MnO) and iron oxide ( $Fe_2O_3$ ). All of those oxides were prepared by self combustion method. Three oxides were then mixed into one mixture oxide using conventional ball milling process by adding 5 mL acetone. The process took 24 h. After that, the mixture was dried in an oven at 110°C to evaporate acetone and the sample was annealed at 700°C for 4 h. This sample was labeled as 700 BM.

**Preparation of  $Mn_{0.8}Zn_{0.2}Fe_2O_4$  by self combustion method:**

The precursor for  $Mn_{0.8}Zn_{0.2}Fe_2O_4$  was prepared by mixing  $Mn(NO_3)_2 \cdot 4H_2O$ ,  $Zn(NO_3)_2 \cdot 6H_2O$  and  $Fe(NO_3)_3 \cdot 9H_2O$  with of 65%  $HNO_3$ . As-prepared samples were stirred for 1 week and gradually heating until combustion occur at 110°C. The sample was then dried in an oven at 110°C for 24 h and annealed at 700°C in argon for 4 h. This sample labeled as 700 SC.

**Sample characterization:** The as-synthesized nanocatalysts were characterized by using X-Ray Diffraction (XRD), Field Emission Scanning Electron Microscopy (FESEM), Energy Dispersive X-ray Spectroscopy (EDX). XRD was used for the identification of phases, crystallinity and crystallite size determination.

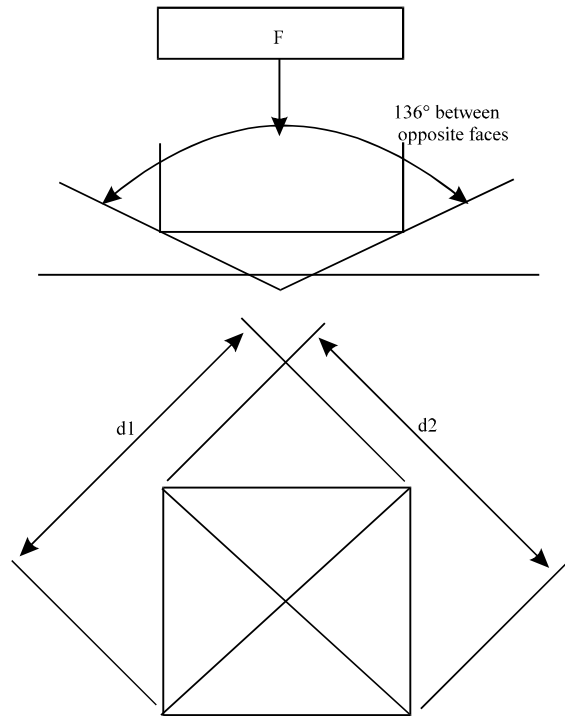


Fig. 1: Vickers microhardness geometry (Callister, 2001)

The FESEM (SUPRA 35VP) gives the microstructure evaluation on the sintered powder. Temperature Program Reduction (TPR) was done using TPDR0 1100 series to determine the activation energy of the sintered sample  $Mn_{0.8}Zn_{0.2}Fe_2O_4$  when it was reduced to its metal state.

**Mechanical properties:** The mechanical properties (microhardness testing) of  $Mn_{0.8}Zn_{0.2}Fe_2O_4$  was accomplish using Microhardness Vickers LECO LM247AT. The sample was formed into a pellet by using autopellet press machine. The diameter of the pellet was 1 and 0.25 cm thickness.

Microhardness vickers value follow to Eq. 1 (Callister, 2001), (Fig. 1).

$$HV = \frac{2F \sin \frac{136^\circ}{2}}{d^2} = 1.854 \frac{F}{d^2} \tag{1}$$

Where:

HV = Hardness Vickers

F = Load (kgf)

d = Mean of  $d_1$  and  $d_2$  in mm

**Magnetic properties:** The magnetic properties (initial permeability and relative loss factor) of the

$Mn_{0.8}Zn_{0.2}Fe_2O_4$  is determined using Agilent 4294A Impedance Analyzer. The sample was formed into a toroid shape with inner diameter ( $d_1$ ) 0.25 cm, outer diameter ( $d_2$ ) 0.5 and the thickness 0.25 cm.

The value of initial permeability is obtained by using the Eq. 2 (Agilent Technology Japan, 2003).

$$\mu_i = \frac{2\pi L_s}{\mu_0 N^2 t \ln\left(\frac{d_2}{d_1}\right)} \quad (2)$$

Where:

- t = Thickness (m)
- d1 = Inner diameter (m)
- d2 = Outer diameter (m)
- N = Number of winding (20)
- $\mu_0$  = Permeability constant =  $4\pi \times 10^{-7}$  H/m

Relative Loss Factor (RLF) was determined using the following equation:

$$RLF = \frac{1}{\mu_i Q} \quad (3)$$

Where:

- $\mu_i$  = Initial permeability (H/m)
- Q = Q factor

**Temperature Program Reduction (TPR):** TPR investigations were carried out at a heating rate of  $5^\circ C \text{ min}^{-1}$ . The reactive gas composition is hydrogen (5 vol %) in nitrogen. The flow rate was fixed at  $20 \text{ cc min}^{-1}$ . The total reactive gas consumption during TPR analysis was measured. The TPR measurement was carried out following activation after cooling the sample in nitrogen flow to  $40^\circ C$ . Sample was then held at  $1000^\circ C$  for 10 min. The TPR experiment was performed at temperature  $800^\circ C$ .

## RESULTS AND DISCUSSION

**X-ray diffraction result:** X-ray diffraction (XRD) analysis was performed on all sample using Philips X-Ray Diffractometer using  $CuK\alpha$ , with  $\lambda = 1.5406 \text{ \AA}$ . The scanning angles ( $2\theta$ ) were operated from  $10$  to  $80^\circ$  and the speed of the counter was  $0.02^\circ/2\theta$  per min.

The X-Ray Diffraction (XRD) patterns are shown in Fig. 2 for 700 BM and Fig. 3 for 700 SC. The unit cell size and geometry were resolved from the angular positions of the diffraction peaks, whereas the arrangement of the atoms within the unit cell is associated with the relative intensities of these peaks. Figure 2 shows that many noise

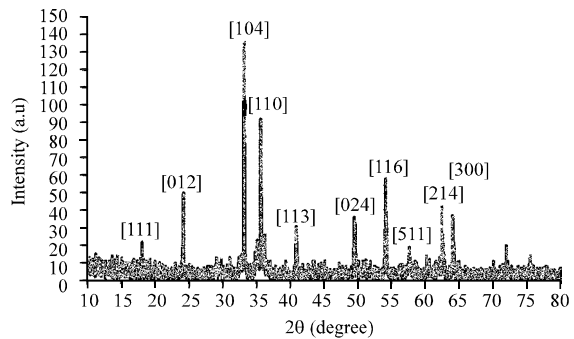


Fig. 2: XRD pattern for 700 BM

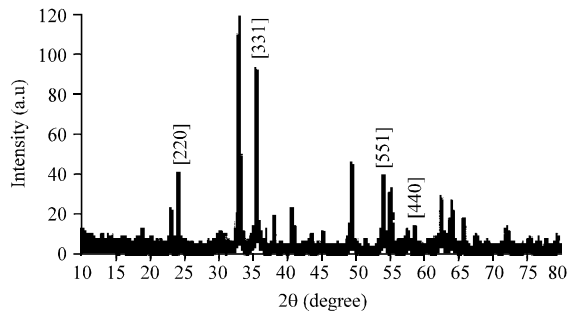


Fig. 3: XRD pattern for 700 SC

and impurities as evident in the as-synthesis sample. It is speculated that the octahedral sites of  $Fe^{2+}$  is not occupying the tetrahedral sites of  $Mn^{2+}$  and  $Zn^{2+}$  (University of Delaware, 2010). Figure 3 shows that there is less impurity. There is one peak that does not coincide with the  $Mn_{0.8}Zn_{0.2}Fe_2O_4$  standard peak. It is because use low temperature, otherwise the matching would have been perfectly show for the single phase  $Mn_{0.8}Zn_{0.2}Fe_2O_4$ .

Table 1 shows the values of Full Width Half Maxima (FWHM), d spacing and crystallite size for the (311) plane. Scherer's equation is used to determine the diameter of manganese zinc ferrite nano-particles by using XRD results. It shows that 700 BM has bigger crystallite size (125.6) than 700 SC (31.8 nm). From the standard card SS-NNNN 89-6609 the structure of 700 BM is cubic structure and from SS-NNNN 74-2401 the structure of 700 SC is cubic structure.

**Field emission scanning electron microscope result:** Figure 4 shows the nanoparticle of  $Mn_{0.8}Zn_{0.2}Fe_2O_4$  prepared by conventional ball milling method annealed at  $700^\circ C$  possessing size particles in the range of 14-26 nm. While Fig. 5 shows the nanoparticles of  $Mn_{0.8}Zn_{0.2}Fe_2O_4$  annealed at  $700^\circ C$  by self combustion technique with the range of dimensions 64-87 nm.

Table 1: Comparative values of intensity, FWHM, d-spacing, crystallite size of 700 BM and 700 SC

Samples	X-ray diffraction (Correspond to [311] peaks)					
	FWHM	d-spacing (Å)	Crystallite esize (nm)	a	b	c
700 BM	0.066	2.417	125.6	8.4551	8.4551	8.4551
700 SC	0.259	2.694	31.8	8.4975	8.4975	8.4975

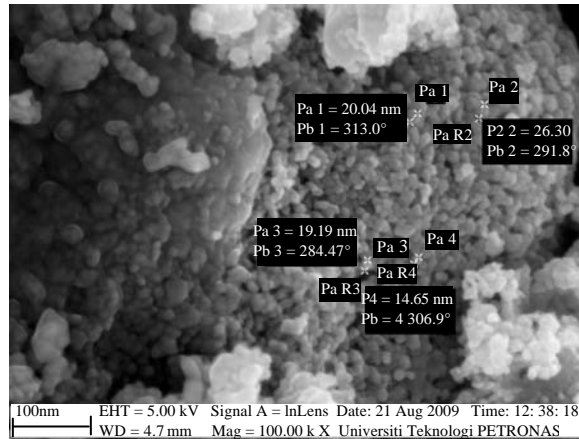


Fig. 4: FESEM morphology 700BM

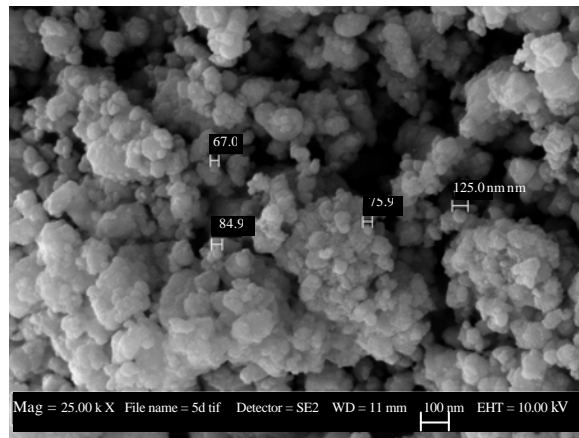


Fig. 5: FESEM morphology of 700SC

**Energy Dispersive X-Ray (EDX) result:** From the EDX analyses, we see evidence of Mn, Zn, Fe and O. Table 2 shows the relative abundance of each of the element to be comparable to the theoretical stoichiometric values. The relative abundant of each element is comparing to the theoretical values Mn = 11.42, Zn = 2.86, Fe = 28.57 and O = 57.14%.

**Microhardness testing:** Materials evaluation and engineering Inc (2010) define that mechanical properties was done using microhardness testing. Microindentation hardness testing (or microhardness testing) is a method

for measuring the hardness of a material on a microscopic scale. A precision diamond indenter is impressed into a pellet of  $Mn_{0.8}Zn_{0.2}Fe_2O_4$  as per ASTM E 384.

Figure 6 shows that 700 SC sample has higher hardness vickers number (75.83 HVN) compared to 700 BM sample. From XRD result as seen in Fig. 2, 700 BM sample has many noise and impurities. Rashad (2006) has been reported that the imperfections within the nano dimension will migrate to the surface to relax themselves under annealing, purifying the material and leaving perfect material structures inside the nanomaterials. Since the annealing process still resulting the impurities within the

Table 2: Comparison of percentage weight and atom 700 BM and 700 SC

Sample	Mn	Zn	Fe	O
<b>700 BM</b>				
Weight %	20.89	15.77	22.24	1.13
Atomic %	10.59	6.72	11.07	71.61
<b>700 SC</b>				
Weight %	6.51	1.20	4.35	2.68
Atomic %	6.48	4.61	28.58	60.33

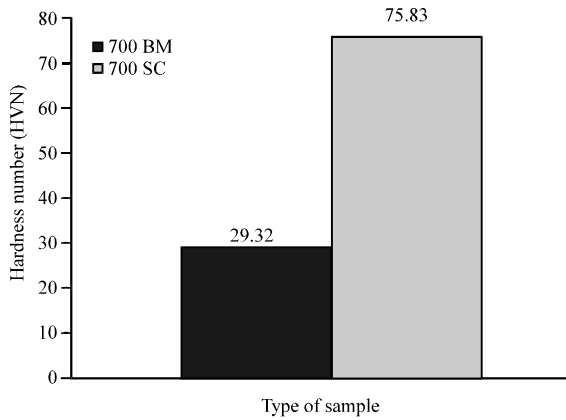


Fig. 6: Comparison of hardness vickers numbers shows the highest value for 700S

sample, it cause low hardness for 700 BM sample. Self combustion method, which has less impurities, resulting higher hardness and better mechanical properties. It has been reported that mechanical properties of manganese zinc ferrite are dependent on the grain size (Baumgartner *et al.*, 1997). Table 1 shows that the crystallite size of 700 SC sample is smaller (31.8) than 700 BM sample (125.6 nm). It can be related that the smaller particle size will provide higher hardness number, in this case hardness number for 700 SC sample increase 155% comparing to 700 BM sample.

**Permeability test:** Studies on magnetic properties of the  $Mn_{0.8}Zn_{0.2}Fe_2O_4$  was performed by using Agilent 4294A Impedance Analyzer. Initial permeability of sample 700 BM and 700 SC was conducted. Figure 7, it was found that sample 700 SC shows higher initial permeability ( $2.5 \times 10^3$ ) compared to its counterpart sample 700 BM which has  $1 \times 10^3$ . There is almost 250% increasing permeability. It is notable that the initial permeability is very much extrinsic, microstructure-sensitive.

Referring to the XRD result as seen in Fig. 2, sample 700 BM has a lot of noise and impurities, therefore the permeability has decreasing. From the morphological view (Table 1), sample 700 BM has bigger crystallite size (125.6 nm) comparing to sample 700 SC with crystallite size 31.8 nm. These result can be related with the magnetic

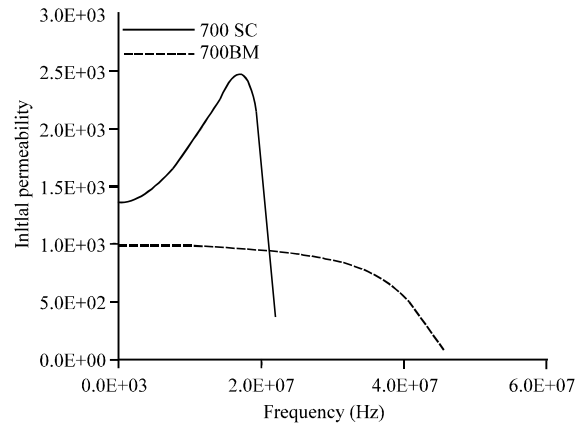


Fig. 7: Comparison of initial permeability for 700BM and 700SC

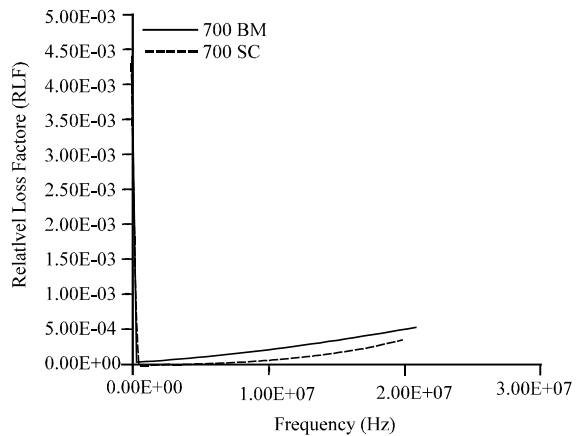


Fig. 8: Comparison of Relative Loss Factor (RLF) for 700 BM and 700 SC

properties, which show that the smaller particle size has higher permeability. Observing the Relative Loss Factor (RLF) at Fig. 8, for the both samples, the sample 700 SC has 10% lower loss factor. It is also related with the structure and morphology of both sample. Many impurities and bigger crystallite size will resulting high loss factor.

**Temperature Program Reduction (TPR) result:** The TPR profiles were presented in Fig. 9 and 10. The purpose is to analyze the reduction temperature for  $Mn_{0.8}Zn_{0.2}Fe_2O_4$  to produce its metallic state. Figure 9 shows the TPR result for 700 BM. There are three peaks that show the reduction of  $Mn_{0.8}Zn_{0.2}Fe_2O_4$  to metallic iron (Fe). The first peak is 484°C, the second peak is 573°C and the third peak is 877°C. The first peak indicates the reduction of MnO to Mn metallic, while the second peak indicates the reduction of  $Fe_2O_3$  to FeO and the third peak indicates the reduction peak to Fe metallic.

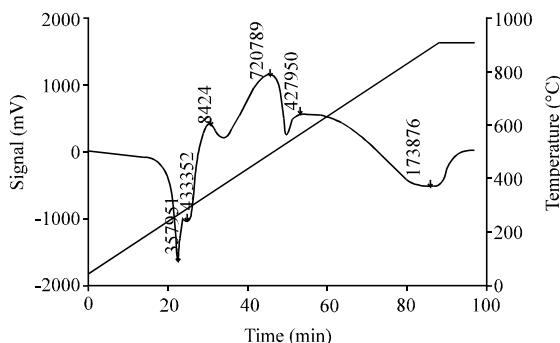


Fig. 9: TPR result for 700 BM

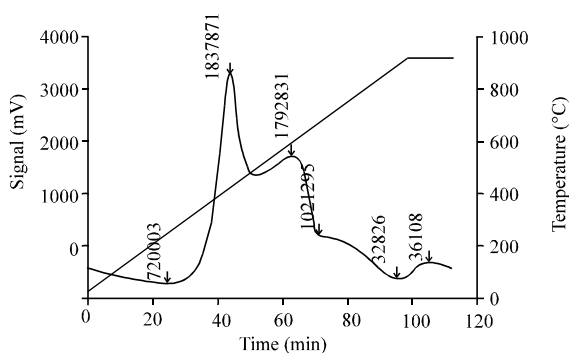


Fig. 10: TPR result for 700 SC

Figure 10 shows the TPR result for sample 700 SC. There are two peaks appearing of 650, 970°C. First peak indicate the temperature reduction for Fe<sub>2</sub>O<sub>3</sub> to FeO and MnO to Mn metallic, while at the second peak indicate the temperature reduction to metallic iron. Temperature reduction for MnO usually occurs at 440-475°C (Khan and Smirniotis, 2008; Bezemer *et al.*, 2006), while temperature reduction for Fe<sub>2</sub>O<sub>3</sub> to Fe<sub>3</sub>O<sub>4</sub> and FeO and Fe at above 394, 545°C (Liang *et al.*, 2009). The temperature reduction for ZnO to Zn metallic is accomplished at 550°C. Above 900°C, it is speculated that all the oxide is reduced to elemental iron (Khan and Smirniotis, 2008).

### CONCLUSION

Mn<sub>0.8</sub>Zn<sub>0.2</sub>Fe<sub>2</sub>O<sub>4</sub> synthesized by conventional ball milling method and self combustion method. Mn<sub>0.8</sub>Zn<sub>0.2</sub>Fe<sub>2</sub>O<sub>4</sub> by self combustion method has better mechanical properties (75.83 HVN) and better magnetic properties due to the high permeability (2.5×10<sup>3</sup>) and 10% lower loss factor comparing with Mn<sub>0.8</sub>Zn<sub>0.2</sub>Fe<sub>2</sub>O<sub>4</sub> by conventional ball milling method. Hence, Mn<sub>0.8</sub>Zn<sub>0.2</sub>Fe<sub>2</sub>O<sub>4</sub> by self combustion method is a better material for ammonia catalyst.

### ACKNOWLEDGMENTS

The authors acknowledge the Ministry of Science and Technology Malaysia for the E-Science research fund (code 03-02-02-sf0031). We would also like to thank to technicians of the Electrical and Electronics, Chemical, and Mechanical Department Universiti Teknologi PETRONAS. For all friends thank you for your kindness cooperation and to those who have given construction comments and idea to completing this paper.

### REFERENCES

- Agilent Technology Japan, 2003. Agilent 4294A Precision Impedance Analyzer Operation Manual. 7th Edn., Kobe Instrument Division, Hyogo, Japan.
- Baumgartner, H., J. Dreikorn, R. Dreyer, L. Michalowsky, E. Pippel and J. Woltersdorf, 1997. Manganese-zinc-ferrites with improved magnetic and mechanical properties. *J. Phys. IV France*, 7: C1-67-C1-68.
- Berdikov, V.F., N.I. Bogomolov, O.I. Pushkarev and V.V. Gavrichenko, 1983. Brittle and strength properties of hot-pressed manganese zinc ferrites by the microindentation method. *Poroshkovaya Metallurgiya*, 8: 87-91.
- Bezemer, G.L., P.B. Radstake, U. Falke, H. Oosterbeek, H.P.C.E. Kuipers, A.J. van Dillen and K.P. de Jong, 2006. Investigation of promoter effects of manganese oxide on carbon nanofiber-supported cobalt catalysts for fischer-tropsch synthesis. *Catalysis*, 237: 152-161.
- Callister, W.D., 2001. *Fundamentals of Material Science and Engineering*. John Wiley and Sons, New York.
- Emad, M., M. Ewais, M.M. Hessien and A.H.A. El-Geassy, 2008. In situ synthesis of magnetic mn-zn ferrite ceramic object by solid state reaction. *J. Aust. Ceramic Soc.*, 44: 57-60.
- Kazemi, S. and G. Fantozzi, 2006. Mechanical spectroscopy of Mn-Zn ferrite. *Mater. Sci. Eng. A*, 442: 496-499.
- Khan, A. and P.G. Smirniotis, 2008. Relationship between temperature-programmed reduction profile and activity of modified ferrite-based catalysts for WGS reaction. *Mol. Catal. A: Chem.*, 280: 43-51.
- Liang, M., W. Kang and K. Xie, 2009. Comparison of reduction behavior of Fe<sub>2</sub>O<sub>3</sub>, ZnO and ZnFe<sub>2</sub>O<sub>4</sub> by TPR technique. *Natl. Gas Chem.*, 18: 110-113.
- Nalbandian, L., A. Delimitis, V.T. Zaspalis, E.A. Deliyanni, D.N. Bakoyannakis and E.N. Peleka, 2008. Hydrothermally prepared nanocrystalline Mn-Zn ferrites: Synthesis and characterization. *Microporous Mesoporous Mater.*, 114: 465-473.

- Ni, S.M. and K.T. Lwin, 2008. Production of Manganese-Zinc Ferrite Core for Electronic Applications. World Academy of Science, Engineering and Technology, Malaysia.
- Rashad, M.M., 2006. Synthesis and magnetic properties of manganese ferrite from low grade manganese ore. *Mater. Sci. Eng. B*, 127: 123-129.
- Sun, K., Z. Lan, Z. Yu, L. Li, H. Ji and Z. Xu, 2009. Effects of nio addition on the structural, microstructural and electromagnetic properties of manganese-zinc ferrite. *Mater. Chem. Phys.*, 113: 797-802.
- University of Delaware, 2010. UD art conservation team restores, preserves historic murals. February 1, 2010. <http://www.udel.edu/udaily/2010/feb/smyrna020110.html>.
- Zuo, X., A. Yang, S.D. Yoon, J.A. Christodoulides, V.G. Harris and C. Vittoria, 2005. Magnetic properties of manganese ferrite films grown at atomic scale. *Applied Phys.*, 97: 10g103-10g103-3.